ISSN 1392–1207. MECHANIKA. 2020 Volume 26(4): 311–317

ANFIS-PID Control of Active Suspension for the Full-Scale Straddle Monorail Model

Liang XIN*, Zixue DU, Junchao ZHOU*****
**Institute of Urban Rail, Chongqing Jiaotong University, Chongqing 400074, P. R. China, E-mail: xinlaero@163.com*
***Institute of Urban Rail, Chongqing Jiaotong University, Chongqing 400074, P. R. China,*
E-mail: aaadzx@163.com (Corresponding Author)
****Institute of Urban Rail, Chongqing Jiaotong University, Chongqing 400074, P. R. China*

crossref http://dx.doi.org/10.5755/j01.mech.26.4.24286

1. Introduction

With the development of cities, urban traffic problems become more and more serious, which needs to adopt new transportation systems. The straddle-type monorail system, as a unique urban rail transit system, has a lot of advantages such as strong climbing ability, small turning radius, fast running speed, small occupied area, safety and comfort, low noise and low cost, so that it is widely applied [1-2]. At present, Chongqing Rail Transit Line 3 is the straddle-type monorail transportation line with the highest transportation efficiency, the longest single-line operation mileage and the most complex topographic conditions in the world.

Suspension system is an important part of monorail vehicles, which guarantees ride comfort. However, its fixed stiffness and damping make it difficult to adapt to complex road conditions. Compared with passive suspension, active suspension can generate instantaneous different active control forces according to the vehicle motion state and road excitation at each moment, so that the suspension is always in the optimal vibration reduction state. Therefore, active suspension has become a hotspot of current research. A lot of control strategies have been studied for active suspension by many researchers.

Hać [3] applies the optimal control theory to the active control of 2-DOF vehicle suspension system, the results show that driving comfort, vehicle safety and suspension travel were fully considered. H_∞ control is proposed by Doyle et al. [4] in 1980s, and then Yamashita et al. [5] design H_∞ controller for the 7-DOF vehicle, which improves the stability of the closed-loop system. Ahmed et al. [6] develop the PID control algorithm for 1/4 car 2-DOF suspension systems, which improves performance of the system with respect to design goals compared to passive suspension system. However, considering the inherent nonlinear of suspension system, such as nonlinear spring and damping, the above linear control strategy is difficult to achieve better results, so many nonlinear control algorithms have been proposed one after another. Chen et al. [7] propose an adaptive sliding controller for controlling a non-autonomous 1/4 car suspension system with time-varying loadings, the results of simulation indicate the proposed controller gives significant performance improvement compared with the pure passive design from the viewpoint of ride comfort. Based on robust sliding mode control, Qin et al. [8] use ICA evolutionary algorithm to optimize the vertical acceleration of passengers. Yoshimura [9-10] has done a lot of research on the fuzzy control of active suspension and semi-active suspension and achieves satisfactory results. Moran and Nagai [11-13] use neural network to identify and control the actual nonlinear suspension, and compare it with the linear controller, that results show the superiority of neural network control. Kumar et al. [14] design an adaptive neural fuzzy inference system (ANFIS) controller, the simulation is carried out for sinusoidal road profile where the body displacement and pitch angle of ANFIS controlled active suspension system is significantly less compare to PID controlled suspension system. Gandhi et al. [15] use a 1/2 active suspension mode to compare the controller such as PID, LQR, FUZZY and ANFIS, the simulation indicates ANFIS controller performed better.

Above of reference, the performance of vehicle suspension system is improved, but all of them are based on simplified mathematical models, i.e. 1/4 model, 1/2 model, 7-DOF model which are quite different from the full-scale model. At the same time, there are few reports on straddle-type monorail active suspension.

Therefore, based on the 38-DOF full-scale dynamic model of straddle-type monorail vehicle, an ANFIS-PID controller is proposed for the whole vehicle in this paper, which uses the modular control thought and adaptive neural fuzzy inference system(ANFIS), then vibration reduction effect of ANFIS-PID controller is studied.

This paper is organized as follows: the 38-DOF full-scale dynamic model with active suspension is established in Section 2, including longitudinal motions, lateral motions, vertical motions, rolling motions, pitching motions and yawing motions. Section 3 designs an ANFIS-PID controller for the whole vehicle, which uses the modular control thought and ANFIS. Section 4 describes the simulation and its result of the proposed controller. Section 5 concludes this paper.

2. Full-scale dynamic model with active suspension

2.1. Monorail vehicle model

The dynamic model of straddle-type monorail vehicle includes 3 parts, i.e. 1 vehicle body and 2 bogies. Each bogie has 4 driving wheels, 4 steering wheels and 2 stabilizing wheels, as shown in Fig.1. The central suspension system consisting of air spring, shock absorber, rubber traction equipment, lateral stopper and actuator is connected in the longitudinal, lateral and vertical direction between the vehicle body and the front and rear bogies, respectively. In the

dynamic model for monorail vehicles, the 6 freedom of vehicle body and 2 bogies, including longitudinal motions, lateral motions, vertical motions, rolling motions, pitching motions and yawing motions, and the 1 rotation freedom of wheel, are taken into consideration. The degree of freedom of the monorail vehicle is shown in Table 1.

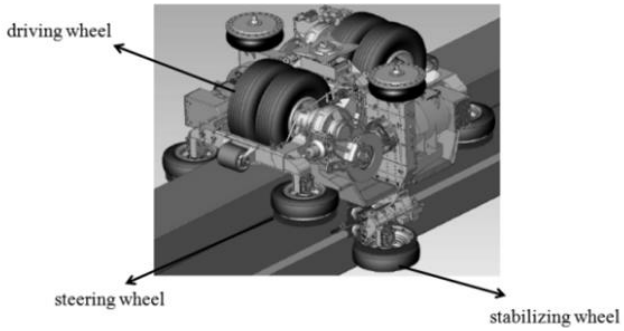

Fig. 1 Bogie model of straddle monorail

The degree of freedom of the monorail vehicle is 38. The dynamic model of is illustrated in Fig. 2, which parameters are shown in reference [1].

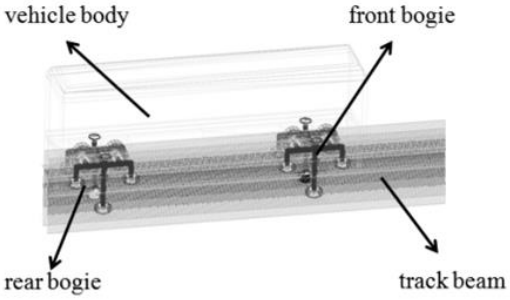

Fig. 2Full-scale dynamics model of straddle monorail

Based on Lagrange Equation, the equations of motion of the vehicle can be described as follow:

$$\frac{d}{dt}\left(\frac{\partial T}{\partial \dot{q}_j}\right)-\frac{\partial T}{\partial q_j}+\frac{\partial U^e}{\partial q_j}+\frac{\partial U^q}{\partial \dot{q}_j}=Q_j, \tag{1}$$

where: T is kinetic energy; U^e is elastic potential energy;

Table 1

The degree of freedom of the monorail vehicle

Vehicle parts(number)	Longitudinal	Lateral	Vertical	Rolling	Pitching	Yawing
Vehicle body (1)	x_c	y_c	z_c	θ_c	ϕ_c	φ_c
Front bogie (1)	x_{t1}	y_{t1}	z_{t1}	θ_{t1}	ϕ_{t1}	φ_{t1}
Rear bogie (1)	x_{t2}	y_{t2}	z_{t2}	θ_{t2}	ϕ_{t2}	φ_{t2}
Driving wheel (4)	-	-	-	-	ϕ_{zij}	-
Steering wheel (4)	-	-	-	-	-	φ_{dij}
Stabilizing wheel (2)	-	-	-	-	-	θ_{dij}

U^q is damping potential energy; Q_j is the generalized forces and moments; q_j is generalized coordinates; $\dot{(\ )}$ denotes the derivative with respect to time.

Equations of kinetic energy, elastic potential energy, damping potential energy and generalized forces and moments are expressed by Eqs. (2) – (5).

$$T=\frac{1}{2}\left\{\begin{array}{l} m_c\left(\dot{x}_c^2+\dot{y}_c^2+\dot{z}_c^2\right)+I_{c\theta}\dot{\theta}_c^2+I_{c\phi}\dot{\phi}_c^2+I_{c\varphi}\dot{\varphi}_c^2+\sum_{i=1}^{2}\left(m_{ti}\left(\dot{x}_{ti}^2+\dot{y}_{ti}^2+\dot{z}_{ti}^2\right)+I_{t\theta i}\dot{\theta}_{t\theta i}^2+I_{t\phi i}\dot{\phi}_{t\phi i}^2+I_{t\varphi i}\dot{\varphi}_{t\varphi i}^2\right)+ \\ +\sum_{i=1}^{2}\sum_{j=1}^{4}\left(I_{z\phi ij}\dot{\phi}_{z\phi ij}^2+I_{d\varphi ij}\dot{\varphi}_{d\varphi ij}^2\right)+\sum_{i=1}^{2}\sum_{j=1}^{2}I_{w\varphi ij}\dot{\varphi}_{w\varphi ij}^2 \end{array}\right\}, \tag{2}$$

$$U^e=\frac{1}{2}\left\{\sum_{i=1}^{2}\sum_{j=1}^{2}\left(K_{kij}^l\left(R_{kij}^l\right)^2+K_{kij}^h\left(R_{kij}^h\right)^2+K_{kij}^v\left(R_{kij}^v\right)^2\right)+\sum_{i=1}^{2}\sum_{j=1}^{4}\left(K_{zij}R_{zij}^2+K_{dij}R_{dij}^2\right)+\sum_{i=1}^{2}\sum_{j=1}^{2}K_{wij}R_{wij}^2\right\}, \tag{3}$$

$$U^q=\frac{1}{2}\left\{\sum_{i=1}^{2}\sum_{j}^{2}\left(C_{kij}^l\left(R_{kij}^l\right)^2+C_{kij}^h\left(R_{kij}^h\right)^2+C_{kij}^v\left(R_{kij}^v\right)^2\right)+\sum_{i=1}^{2}\sum_{j=1}^{4}\left(C_{zij}R_{zij}^2+C_{dij}R_{dij}^2\right)+\sum_{i=1}^{2}\sum_{j=1}^{2}C_{wij}R_{wij}^2\right\}, \tag{4}$$

$$Q_j=\sum_{j=1}^{4}f_j\,. \tag{5}$$

In Eqs. (2)-(5), $R_{kij}^l, R_{kij}^h, R_{kij}^v$ denote the displacement at spring in longitudinal, lateral and vertical direction, R_{zij}, R_{dij}, R_{wij} indicate the displacement of the track beam at the position of driving wheel, steering wheel and stabilizing wheel, f_j is the actuator force,subscript i is the bogie position of the vehicle (i=1, 2 are the front and rear bogies), j is the wheel position in a bogie (j=1, 2, 3, 4 are the front-left, front-right, rear-right, front-right wheels, j=1, 2 are the front and rear wheels), all the other parameters are shown in Table 2.

The actuator force developed by hydraulic actuator is expressed by the nonlinear Eq. (6):

$$\dot{f}_j=-\beta f_j-\alpha A_a^2(\Delta\dot{z})+\Gamma A_a x_v\sqrt{P_s-\mathrm{sgn}(x_v)f_j/A_a}\,. \tag{6}$$

Table 2

The other parameters of straddle monorail dynamics model

Descriptions	Notations
Mass (vehicle and bogie)	m_c, m_{ti}, i = 1,2
Spring constant of air suspension(longitudinal)	$K^{l}_{kij}, i=1,2, j=1,2,3,4$
Spring constant of air suspension(lateral)	$K^{h}_{kij}, i=1,2, j=1,2,3,4$
Spring constant of air suspension(vertical)	$K^{v}_{kij}, i=1,2, j=1,2,3,4$
Spring constant of driving wheel	K_{zij}, i = 1, 2, j = 1,2,3,4
Spring constant of steering wheel	K_{dij}, i = 1, 2, j = 1,2,3,4
Spring constant of stabilizing wheel	K_{wij}, i = 1, 2, j = 1,2
damping constant of air suspension(longitudinal)	$C^{l}_{kij}, i=1,2, j=1,2,3,4$
Damping constant of air suspension(lateral)	$C^{h}_{kij}, i=1,2, j=1,2,3,4$
damping constant of air suspension(vertical)	$C^{v}_{kij}, i=1,2, j=1,2,3,4$
damping constant of driving wheel	C_{zij}, i = 1, 2, j = 1,2,3,4
damping constant of steering wheel	C_{dij}, i = 1, 2, j = 1,2,3,4
damping constant of stabilizing wheel	C_{wij}, i = 1, 2, j = 1,2
Massmomentsofinertia	$I_{c\theta}, I_{c\phi}, I_{c\varphi}, I_{t\theta i}, I_{t\phi i}, I_{t\varphi i}, I_{z\phi ij}, I_{d\varphi ij}, I_{w\varphi ij}$

2.2. Curving track beam model

Considering the transition curve, longitudinal gradient, curve super elevation, indirect track joints and track turnout structure, a track beam model is established, which consists of three sections: the 1st section is a 100m straight line section, the 2nd section is a curve section with a curvature radius of 100 m, an included angle of 60° and a super elevation of 40.8 mm, and the last section is a 100m straight line section, respectively, as shown in Fig. 3 and Table 3.

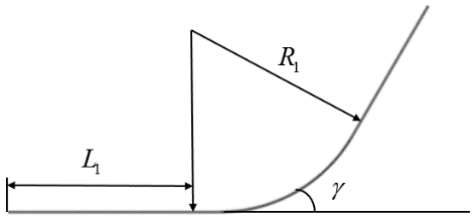

Fig. 3 Curving track beam model

According to the ISO8608[16], the pavement power spectral density(PSD) can be expressed as follows:

$$G_q(\Omega)=\frac{\alpha}{\Omega^n+\beta^n}=G_q(\Omega_0)\left(\frac{\Omega_0}{\Omega}\right)^{-n}, \tag{7}$$

where: Ω is spatial Frequency; n is frequency index.

3. Design of control algorithms of full-scale model

According to the modular control thought [17], the vehicle is decomposed into vertical motion, pitching motion and rolling motion, which are important evaluation indexes of ride comfort. Then three independent ANFIS-PID controllers are established for this three motion, in which the vertical vibration velocity and acceleration, pitching angular velocity and angular acceleration, rollingangular velocity and angular acceleration are taken as inputs and the actuator forceof active suspensionas outputs.

3.1. Pseudo-inverse matrix method

In order to realize the coordinated control of the actuator force of active suspension, the pseudo-inverse matrix method is used, and the 38-DOF ANFIS-PID control structure of the vehicle is obtained, as shown in Fig. 4, where $\dot{z}$ and $\ddot{z}$ are the vertical vibration velocity and acceleration, $\dot{\theta}$ and $\ddot{\theta}$ are the pitching angular velocity and angular acceleration, $\dot{\varphi}$ and $\ddot{\varphi}$ are the rolling angular velocity and angular acceleration. Four active suspension control forces of vehicle system can be obtained by dynamic model:

$$\begin{bmatrix} f_1 \\ f_2 \\ f_3 \\ f_4 \end{bmatrix} = \begin{bmatrix} \frac{l_r}{2(l_f+l_r)} & \frac{1}{acos(\theta)} & -\frac{1}{2(l_f+l_r)cos(\phi)} \\ \frac{l_r}{2(l_f+l_r)} & -\frac{1}{acos(\theta)} & -\frac{1}{2(l_f+l_r)cos(\phi)} \\ \frac{l_f}{2(l_f+l_r)} & \frac{1}{acos(\theta)} & \frac{1}{2(l_f+l_r)cos(\phi)} \\ \frac{l_f}{2(l_f+l_r)} & -\frac{1}{acos(\theta)} & \frac{1}{2(l_f+l_r)cos(\phi)} \end{bmatrix} \begin{bmatrix} F_s \\ M_{s\theta} \\ M_{s\phi} \end{bmatrix}. \tag{8}$$

Table 3

The parameters of curving track beam model

Parameters	Length of straight line section L_1/m	Curvature radius of curve section R_1/m	Included angle of curve section γ/°	Track width/m	Side track width/m
Value	100	100	60	0.8	1.5

Therein: f_i(i=1, 2, 3, 4) indicates control forces of four active suspension; F_s is damping force for suppressing vertical vibration; $M_{s\theta}$ is damping moment for suppressing the rolling motion; $M_{s\phi}$ is damping moment for suppressing the pitching motion.

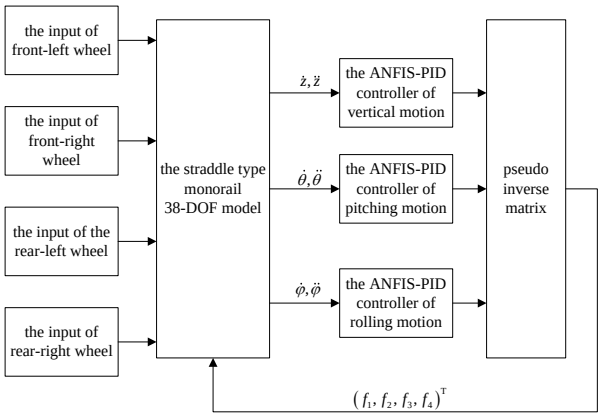

Fig. 4 38-DOF ANFIS-PID control structure

3.2. ANFIS-PID controller

3.2.1. ANFIS theory

The adaptive fuzzy inference system (ANFIS) is a kind of fuzzy inference system based on Takagi-Sugeno model which combines the neural network and the fuzzy logic. According to the information of input-output pairs, the hybrid algorithm can automatically generate IF-THEN rules and realize the online adjustment of membership function.

The ANFIS is comprised of 5 layer architecture, its typical structure is depicted in Fig. 5. The 1st layer gives the degree of membership values. For this paper, the membership function is distinguished into 5 variables, i.e. Negative Big(NB), Negative Small(NS), Zero(ZO), Positive Small(PS), Positive Big(PB), i.e. E_i, R_i, i =1, 2,…,5. The input of the 1st layer is are error x_1=e and change in error values x_2=de/dt. The 2nd layer consists of 25 nodes; each node represents a fuzzy rule. The 3rd layer determines the ratio of the triggering strength of each rule to the sum of the triggering strength of all rules. The output is the triggering strength of each rule after normalization.

$$\bar{w}_k = \frac{w_k}{\sum_{k=1}^{25} w_k}, \tag{9}$$

where: w_k isthe triggering strength of each rule.

The output of each rule is given in the 4th layer.

$$y_k = \bar{w}_k f_k = p_k x_1 + q_k x_2 + r_k, \tag{10}$$

where: f_k is membership function of output variable; p_k, q_k and r_k are coefficient.

The 5th layer is defuzzified layer which calculates the overall output of this layer.

$$y = \sum_{k=1}^{25} \bar{w}_k * y_k. \tag{11}$$

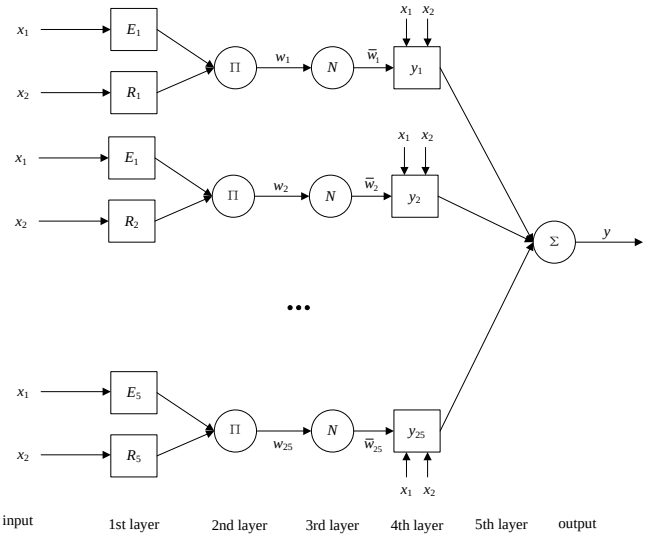

Fig. 5 Typical structure of ANFIS

3.2.2 Design of ANFIS-PID controller

In order to solve the problem that the control effect becomes worse because of the large and fast changing range of the controlled object, ANFIS is used to dynamically adjust the three parameters of PID in the control process, so that the control effect is always in the best state, and its structure is shown in Fig. 6. In Fig. 6, r_{in} is input value, y_{out} is output value, de/dt represents the derivative with respect to time, k_p is proportional coefficient, k_i is integral coefficient, k_d is derivative coefficient.

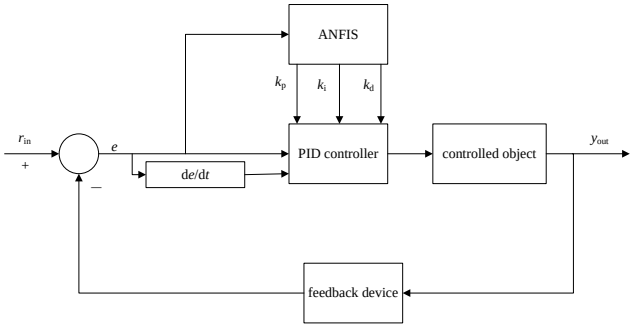

Fig. 6 ANFIS-PID control structure

In order to achieve the desired function of the controller, three ANFIS-PID systems are designed, each of which is a five-layer feedforward neural network. Two variables are selected in the input layer, i.e. error e and change in error values de/dt; five variables are used in each variable language, [NB, NS, ZO, PS, PB], i.e., Negative Big, Nega-

tive Small, Zero, Positive Small and Positive Big; the membership function is Gauss function; the number of design fuzzy rules is $5\times5=25$; and three variables in the output layer, i.e., the parameters k_p, k_i, k_d that need to be tuned.

4. Simulation and result

The simulation uses A-class road, vehiclevelocities is 36km/h and the Runge-Kutta method is used for time advance. The simulation time step is 0.005 s and the total simulation time is 35 s. The fuzzy-PID controller is developed for active suspension in order to compare the result of ANFIS-PID and passive suspension.

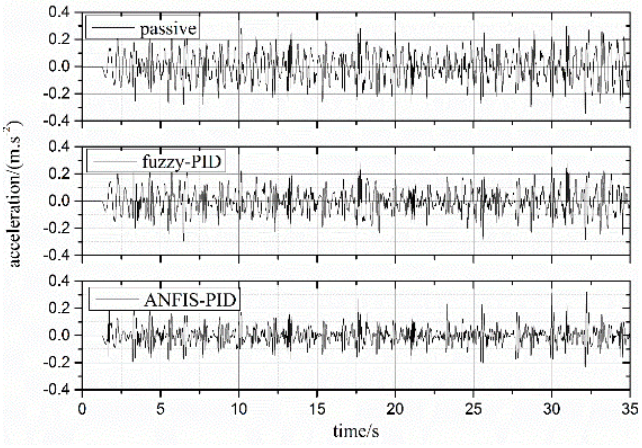

a) Vertical acceleration

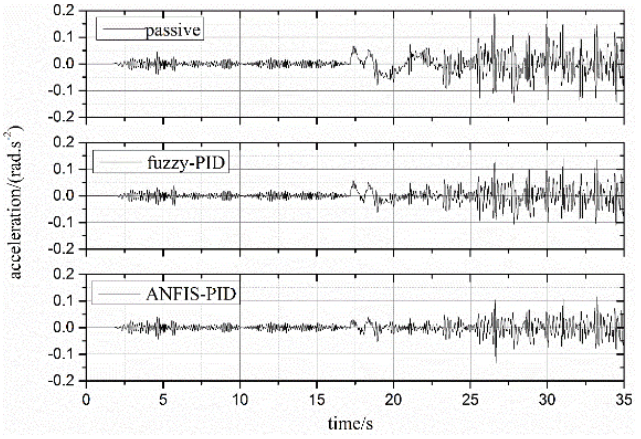

b) Pitching angular acceleration

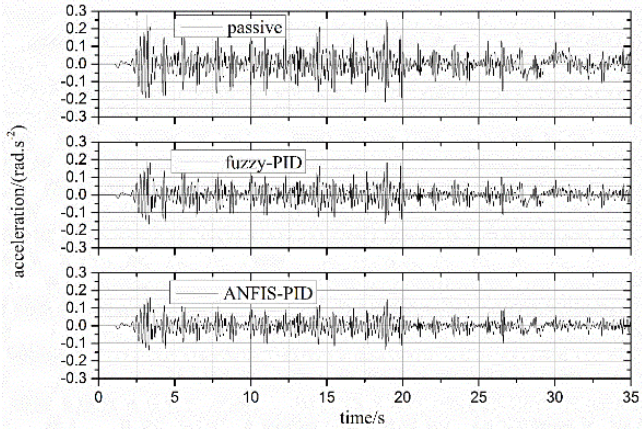

c) Rolling angular acceleration

Fig. 7 Response of vertical acceleration, pitching angular acceleration and rolling angular acceleration

The response of vertical acceleration, pitching angular acceleration and rolling angular acceleration is illustrated in Fig. 7. It can be observed from Fig. 7 thatcompared with passive suspension, the vertical acceleration, pitching angular acceleration and rolling angular acceleration of fuzzy-PIDand ANFIS-PID controlled active suspension system was significantly reduced, and the ANFIS-PID is better. The results show that the two active suspension systems can suppress the vibration of the whole vehicle and improve the ride comfort.

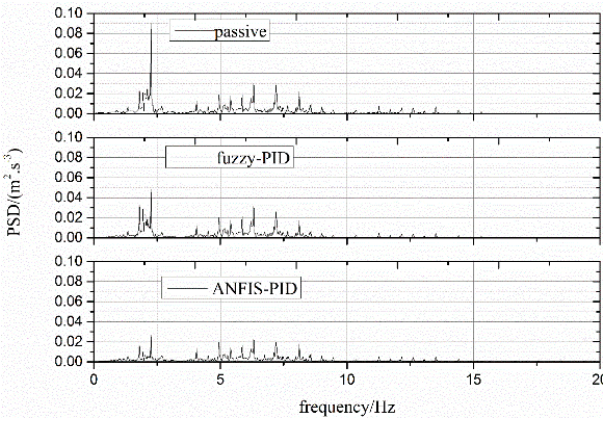

a) Vertical acceleration

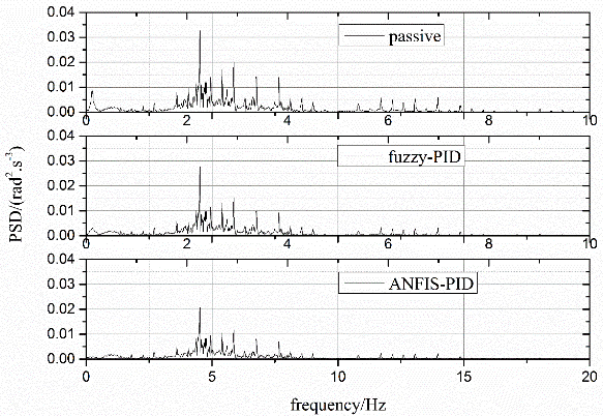

b) Pitching angular acceleration

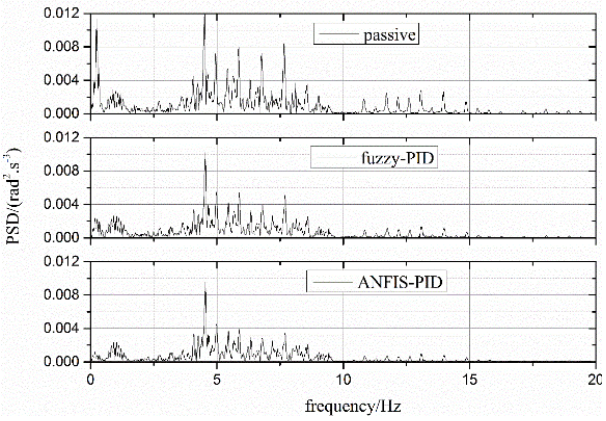

c) Rolling angular acceleration

Fig. 8 PSD of vertical acceleration, pitching angular acceleration and rolling angular acceleration

The power spectral density(PSD) of vertical acceleration, pitching angular acceleration and rolling angular acceleration is represented in Fig. 8. As shown in Fig. 8, the vibration amplitude below 10Hz frequency range is suppressed of fuzzy-PID and ANFIS-PID controlled active suspension system, which is the human sensitivity frequency.

Table 4

The RMS of active suspension and passive suspension

Parameter	Passive suspension	Fuzzy-PID	Reduction, %	ANFIS-PID	Reduction, %
Vertical acceleration	0.1013	0.08463	16.5	0.05995	40.8
Pitching angular acceleration	0.05646	0.04296	23.9	0.03513	37.8
Rolling angular acceleration	0.03248	0.02513	22.6	0.01987	38.8

In order to compare the control effect of active suspension more clearly, Table 4 shows the root mean square (RMS) value comparison of simulation results of vibration of active suspension and passive suspension. The results show that compared with passive suspension, the RMS of vertical acceleration, pitch angle acceleration and roll angle acceleration of active suspension controlled by fuzzy-PID are reduced by 16.5, 23.9 and 22.6%, while the controlled by ANFIS-PID are reduced by 40.8, 37.8 and 38.8%. The ride comfort is also improved by means of the reduction of the acceleration with the help of controller, especially ANFIS-PID controller.

5. Conclusions

Based on the 38-DOF full-scale straddle monorail model, combined with modular control thought and ANFIS control theory, the ANFIS-PID controller is designed to control the vertical motion, pitching motion and rolling motion of vehicle. The simulation results show that the ANFIS-PID controller proposed in this paper is superior to the fuzzy-PID control and passive control, and can effectively improve the ride comfort of vehicle.

Acknowledgments

This work was supported by the National Natural Science Foundation of China (Grant No. 51475062).

References

1. **Wen, X. X.; Du, Z. X.; Zuo C. Y.;** et al. 2014.Influence of cornering stiffness of straddle-type monorail running wheel on tire wear under curve negotiating, Journal of Traffic and Transportation Engineering 14(2): 41-48 (in Chinese). http://dx.doi.org/10.3969/j.issn.1671-1637.2014.02.008.
2. **Matsunaka, R.; Oba,T.; Nakagawa, D.;** et al. 2013. International comparison of the relationship between urban structure and the service level of urban public transportation –A comprehensive analysis in local cities in Japan, France and Germany, Transport Policy30: 26-39. http://dx.doi.org/10.1016/j.tranpol.2013.06.008.
3. **Hać, A.** 1985.Suspension optimization of a 2-DOF vehicle model using a stochastic optimal control technique, Journal of Sound and Vibration 100(3): 343-357. http://dx.doi.org/10.1016/0022-460X(85)90291-3.
4. **Doyle, J. C.; Glover, K.; Khargonekar, P. P.;** et al. 1989. State space solution to standard H_2 and H_∞ control problem, IEEE Transactions on Automatic Control 34(8): 831-847. http://dx.doi.org/10.1109/9.29425.
5. **Yamashita, M.; Fujimori, K.; Hayakawa, K.;** et al. 1994. Application of H_∞ control to active Suspension systems, Automatica 30(11): 1717-1729. http://dx.doi.org/10.1016/s1474-6670(17)48688-5.
6. **Ahmed, A. E. N. S.; Ali, A. S.; Ghazaly, N. M.;** et al. 2015. PID controller of active suspension system for a quarter car model, International Journal of Advances in Engineering & Technology 8(6): 899-909.
7. **Chen, P. C.; Huang, A. C.** 2005. Adaptive sliding control of non-autonomous active suspension systems with time-varying loadings, Journal of Sound and Vibration 282(3-5): 1119-1135. http://dx.doi.org/10.1016/j.jsv.2004.03.055.
8. **Qin, S.; Samuel, A.** 2013. Analysis of robustness sliding mode control method for active suspension system, International Journal of Automation and Control Engineering 2(3): 137-142.
9. **Yoshimura, T.** 1996. Active suspension of vehicle using fuzzy logic, International Journal of System Sciencem 27(2): 215-219. http://dx.doi.org/10.1080/00207729608929206.
10. **Yoshimura, T.** 1998. A semi-active suspension of passenger cars using fuzzy reasoning and the field testing, International Journal of Vehicle Design 19(2): 150-166. http://dx.doi.org/10.1504/IJVD.1998.062100.
11. **Moran, A.; Nagai, M.** 1993. Optimal preview control of rear suspension using nonlinear neural networks, Vehicle System Dynamics 22(5-6): 321-334. http://dx.doi.org/10.1080/00423119308969034.
12. **Moran, A.; Nagai, M.** 1994. Optimal active control of nonlinear vehicle suspensions using neural networks, JSME International Journal, Series C: Dynamics, Control, Robotics, Design and Manufacturing 37(4): 707-718. http://dx.doi.org/10.1299/jsmec1993.37.707.
13. **Nagai, M.; Moran, A.; Tamura,Y.;** et al. 1997. Identification and control of nonlinear active pneumatic suspension for railway vehicles using neural networks, Control Engineering Practice 5(8): 1137-1144. http://dx.doi.org/10.1016/s0967-0661(97)00107-x.
14. **Kumar, P. S.; Sivakumar, K.; Kanagarajan, R.;** et al. 2018. Adaptiveneuro fuzzy inference system control of active suspension system with actuator dynamics, Journal of Vibroengineering 20(1):541-549. http://dx.doi.org/10.21595/jve.2017.18379.
15. **Gandhi, P.; Adarsh, S.; Ramachandran, K. I.** 2017. Performance analysis of half car suspension model with 4 DOF using PID, LQR, FUZZY and ANFIS controllers, Procedia Computer Science 115:2-13. http://dx.doi.org/10.1016/j.procs.2017.09.070.
16. **Bao, Y.; Li, Y.; Ding, J.** 2016. A case study of dynamic response analysis and safety assessment for a suspended monorail system, International Journal of Environmental Research & Public Health 13(11): 1121. http://dx.doi.org/10.3390/ijerph13111121.
17. **Chen, J. P.** 2011. Whole vehicle magnet rorheological fluid damper semi-active suspension variable universe fuzzy control simulation and test, Transactions of the Chinese Society for Agricultural Machinery 42(5):7-13. http://dx.doi.org/10.4028/www.scientific.net/AMR.211-212.106.

L. Xin, Z. Du, J. Zhou

ANFIS-PID CONTROL OF ACTIVE SUSPENSION FOR THE FULL-SCALE STRADDLE MONORAIL MODEL

S u m m a r y

In order to improve the ride comfort straddle-type monorail, based on the full-scale straddle-type monorail model with 38-DOF, combined with the modular control thought and adaptive neural fuzzy inference system (ANFIS) control theory, the ANFIS-PID controller is designed, in which the vertical vibration velocity and acceleration, pitching angular velocity and angular acceleration, rolling angular velocity and angular acceleration are taken as inputs and the actuator force of active suspension as outputs. The results show that compared with existing passive suspension, the root mean squared values (RMS) of vertical acceleration, pitching angular acceleration and rolling angular acceleration of active suspension is significantly reduced, respectively. And the vibration amplitude below 10 Hz frequency range is suppressed, which is the human sensitivity frequency. Active suspension controlled by ANFIS-PID can be used as a way to improve the ride comfort of straddle monorail vehicles.

Keywords: straddle monorail vehicle, active suspension, full-scale model, ANFIS-PID.

Received September 24, 2019
Accepted August 24, 2020

This article is an Open Access article distributed under the terms and conditions of the Creative Commons Attribution 4.0 (CC BY 4.0) License (http://creativecommons.org/licenses/by/4.0/).